Energetics of asteroid dynamos and the role of compositional convection

F. Nimmo[1]

Received 2 March 2009; revised 10 April 2009; accepted 16 April 2009; published 19 May 2009.

[1] The conditions under which a dynamo can operate in the core of a small planetary body or asteroid are examined. Compositional convection driven by inner core growth is thermodynamically much more efficient than thermal convection at driving a dynamo, but whether asteroid cores crystallize in this fashion is currently uncertain. Inner core solidification will drive dynamo activity in cores larger than $\approx$50–150 km in radius. Dynamo activity requires core cooling rates exceeding $\sim$0.001–0.1 K/My if compositional convection occurs. In the absence of an inner core, cooling rates of $\sim$1–100 K/My or heating by ^{60}Fe within 10–20 Myr of solar system formation are required to drive a dynamo. If inner core growth is important (as for the IVB iron meteorite parent body) then a dynamo should develop with magnetic paleointensities that depend on the core sulphur content. If ^{60}Fe decay is dominant, the frequency of asteroid dynamo occurrence is predicted to decay with distance from the Sun. **Citation:** Nimmo, F. (2009), Energetics of asteroid dynamos and the role of compositional convection, *Geophys. Res. Lett.*, *36*, L10201, doi:10.1029/2009GL037997.

1. Introduction

[2] Many meteorite parent bodies possessed iron cores which were liquid for at least several million years before solidifying [*Chabot and Haack*, 2006]. Such liquid cores, if convecting due to thermal or compositional buoyancy, could lead to self-sustaining dynamos resembling the Earth's. It has recently been argued [*Weiss et al.*, 2008] that the observed paleomagnetism of angrite meteorites is most likely due to an early dynamo on the angrite parent body. Here I will argue that compositional buoyancy, if present, is much more efficient than thermal buoyancy at driving dynamos on small bodies, and point out some observational consequences.

[3] Although a great deal of attention has been paid to the Earth's dynamo, theoretical work on small body dynamos has mainly been confined to abstracts [e.g., *Runcorn*, 1994]. Lunar paleomagnetism [*Garrick-Bethell et al.*, 2009] and dynamo activity in the presumed lunar core [*Stegman et al.*, 2003] and Ganymede's sulphur-rich core [*Hauck et al.*, 2006] have been studied in more detail.

2. Core Crystallization

[4] Generation of a dynamo requires a moving conductive liquid. In the case of asteroids, the conductive liquid is the molten iron core, and the duration and strength of the dynamo therefore depend on the cooling and crystallization history of the core.

[5] Hafnium-tungsten isotope data suggest that some iron meteorites differentiated within 1 Myr of solar system formation (defined by the age of CAIs, calcium-aluminium inclusions [*Markowski et al.*, 2006]). The energy source causing this melting was almost certainly ^{26}Al, with a half-life of 0.73 Myr, though ^{60}Fe (half-life 1.5 Myr) may have played a secondary role. Subsequent crystallization of these cores was delayed, and the period over which freezing took place was apparently short compared to the time spent completely molten [*Chabot and Haack*, 2006].

[6] The variable amounts of sulphur thought to be present in asteroid cores [*Chabot*, 2004] leads to uncertainties in how they crystallized. Depending on the relative slopes of the melting curve and the adiabat, crystallization may proceed from the centre upwards or from the outside downwards [*Haack and Scott*, 1992; *Chabot and Haack*, 2006; *Wasson et al.*, 2006]. In the former case, inner core solidification will likely be accompanied by expulsion of a light, sulphur-rich fluid, driving compositional convection. A similar process is thought to operate within the Earth's core. In the latter case, any light fluid expelled will remain at the top of the core and not drive circulation. However, the solidifying material will be likely denser than the surrounding liquid and thus sink and re-melt, potentially driving flow [*Hauck et al.*, 2006]. Apparent fractional crystallization trends for iron meteorites within the same group suggest that the cores were efficiently stirred [*Esbensen et al.*, 1982]. Studies of coupled Ni concentrations and subsolidus cooling rates in iron meteorites suggest top-down crystallization for IIIAB and IVA meteorites, and bottom-up crystallization for IVB's [*Yang and Goldstein*, 2006; *Yang et al.*, 2008, 2009]. In what follows, we will examine the consequences of bottom-up core crystallization (as on Earth), but note that this is likely only relevant to some meteorites.

2.1. Magnetic Reynolds Number

[7] Whether or not a dynamo will operate is determined in large part by the magnetic Reynolds number $Re_m = vL/\eta$, where v and L are the characteristic velocity and length-scale, respectively, and η is the magnetic diffusivity [*Stevenson*, 2003]. A dynamo is likely for $Re_m \geq 10^2$–10^3. The length-scale L is typically taken to be the core radius r_c; the main difficulty in calculating Re_m is therefore in estimating the characteristic velocity.

[8] For purely thermal convection, the velocity depends on the heat flow excess over the adiabatic value and may be estimated using mixing length theory [*Stevenson*, 2003; *Weiss et al.*, 2008]. However, this analysis neglects compo-

[1]Department of Earth and Planetary Sciences, University of California, Santa Cruz, California, USA.

0094-8276/09/2009GL037997$05.00

sitional convection, which can drive a dynamo even if the heat flow is subadiabatic [*Loper*, 1978]. Numerical experiments have shown that the convective velocity depends on the buoyancy flux-based Rayleigh number [*Olson and Christensen*, 2006]. Specifically,

$$\frac{v}{\Omega d} \approx \beta \left(\frac{r_c}{r_i} \frac{g F_b}{\rho} \frac{1}{\Omega^3 d^2} \right)^{2/5} \quad (1)$$

Here β is a constant (= 0.85), r_i is the inner core radius, g is the gravitational acceleration (here evaluated at, and thus proportional to, r_i), ρ is the density, d is the thickness of the convecting layer (= $r_c - r_i$), Ω is the rotation angular frequency and F_b is the buoyancy flux (kg m^{-2} s^{-1}). For compositional convection driven by bottom release of light fluid with a density contrast $\Delta\rho$, we have $F_b = \Delta\rho \frac{dr_i}{dt} \approx \Delta\rho\, r_c/\tau$, where τ is the timescale for inner core growth. Setting $d \approx r_c$ we may rewrite equation (1) as follows:

$$v \approx \beta r_c^{3/5} \Omega^{-1/5} \left(\frac{4\pi G \Delta\rho}{3} \frac{dr_i}{dt} \right)^{2/5} \quad (2)$$

where G is the gravitational constant. Compositional convection is more vigorous for larger density contrasts or more rapidly growing inner cores, but is less vigorous for smaller bodies. Taking reasonable Earth core parameters ($\Delta\rho$ = 300 kg m^{-3}, τ = 1 Gyr, r_c = 3000 km), equation (2) yields velocities of a few mm/s, comparable to inferences based on the observed secular variation of the Earth's magnetic field [e.g., *Holme*, 2007]. We may thus write the magnetic Reynolds number as

$$Re_m \approx \frac{\beta r_c^{8/5}}{\Omega^{1/5} \eta} \left(\frac{4\pi G \Delta\rho}{3} \frac{dr_i}{dt} \right)^{2/5} \approx 40 \left(\frac{r_c}{90\ \text{km}} \right)^2 \left(\frac{10\ \text{Myr}}{\tau} \right)^{2/5} \quad (3)$$

where the second approximation was calculated using η = 2 m^2 s^{-1}, $\Delta\rho$ = 300 kg m^{-3} and $\Omega = 3 \times 10^{-4}$ s^{-1} (6 hr period). Since Re_m = 40 is the critical value for dynamo activity [*Olson and Christensen*, 2006], equation (3) shows that the minimum likely core size for a dynamo driven by compositional convection is ≈90 km, with the largest uncertainties being due to the core solidification timescale τ. This critical radius is very similar to that found by *Weiss et al.* [2008] for thermal convection. In reality, dr_i/dt exceeds r_c/τ when $r_i \ll r_c$; thus, the minimum critical core size deduced here is likely to be an overestimate when the inner core is small.

3. Energy and Entropy Budgets

[9] To determine whether or not a dynamo operates requires consideration of the core entropy and energy budgets [e.g., *Nimmo*, 2007] (hereinafter referred to as N07). This approach neglects the role of rotation, which affects the onset of convection and dynamo activity [e.g., *Christensen and Aubert*, 2006], but does encapsulate much of the basic physics.

[10] The adiabatic temperature $T(r)$ inside a small convecting core is given by *Labrosse* [2003]

$$T(r) = T_c \exp\left[-\left(r^2 - r_c^2 \right) / D^2 \right] \quad (4)$$

where T_c is the temperature at the core-mantle boundary (CMB), r is the radial distance from the centre of the body and D is the scale height given by

$$D = \left(\frac{3 C_p}{2\pi\alpha\rho G} \right)^{1/2} \quad (5)$$

Here C_p is the specific heat capacity and α is the thermal expansivity.

[11] Neglecting small terms, the entropy balance for a convective dynamo may be written (N07)

$$E_\Phi + E_k = E_R + E_s + E_g + E_L \quad (6)$$

[12] The driving terms are: E_R, due to radioactive decay or other internal heat sources; E_s, core cooling; E_g, the gravitational contribution due to light element release during inner core growth; and E_L, latent heat release during inner core growth. The sink terms are E_k, the conductive contribution, and E_Φ, the entropy associated with Ohmic dissipation caused by the dynamo. Equation (6) shows that to drive a more dissipative dynamo, or one in which the conductive contribution is larger, requires either more rapid core cooling, more internal heating or more rapid inner core growth.

3.1. Inner Core Growth

[13] Assuming an Earth-like inner core, the rate of inner core growth $\frac{dr_i}{dt}$ depends on the relative slopes of the solidus, dT_m/dP, and the adiabat, dT/dP. Following N07, we may write

$$\frac{dr_i}{dt} = \frac{T_i}{T_c \left(\frac{dT_m}{dP} \rho g_i - \frac{2 r_i T_i}{D^2} \right)} \frac{dT_c}{dt} \approx \frac{D^2}{2 T_c f r_c (\Delta - 1)} \frac{dT_c}{dt} \quad (7)$$

[14] Here r_i, T_i and g_i are the radius, temperature and gravity at the inner core boundary, and the second equality assumes that $T_i \approx T_c$, $r_i = f r_c$ and $dT/dr = 2rT/D^2$ (equation (4)). The quantity Δ gives the relative slopes of the solidus and adiabat and is given by

$$\Delta = \frac{dT_m/dP}{dT/dP} = \frac{dT_m}{dP} \frac{\rho C_p}{\alpha T_i} \quad (8)$$

where we have made use of equation (5). Equation (7) shows that the more nearly parallel the solidus and the adiabat are (smaller Δ), the more rapid inner core growth is. If $\Delta < 1$ then core solidification occurs at the outer edge of the core and not at the centre (see Discussion below).

3.2. Summary of Relevant Terms

[15] The compressibility of iron means that its density will also vary with radius. However, because the lengthscale of the density variation is larger than D, we will neglect it here and simply assume that density within the liquid part of the core is constant. Doing so introduces only minor errors and considerably simplifies the algebra.

[16] For the specific temperature distribution given in equation (4) and assuming constant density, the entropy contributions E_k, E_R, E_s, and their corresponding power

Table 1. Energy and Entropy Terms Associated With a Cooling and Solidifying Core[a]

	Power (Q)	Entropy (E)
Q_s, E_s	$-M_c C_p \frac{dT_c}{dt}\left[1+\frac{2}{5}\frac{r_c^2}{D^2}\right]$	$-M_c C_p \frac{1}{T_c}\frac{2}{5}\frac{r_c^2}{D^2}\frac{dT_c}{dt}$
Q_R, E_R	$M_c h$	$M_c h \frac{1}{T_c}\frac{2}{5}\frac{r_c^2}{D^2}$
Q_g, E_g	$-3\pi G\rho M_c F \frac{\Delta\rho}{\rho}\frac{1}{\Delta-1}\frac{D^2}{T_c}\frac{dT_c}{dt}$	$\frac{Q_g}{T_c}$
Q_L, E_L	$-\frac{3}{2}M_c\frac{fL_H D^2}{T_c r_c^2}\frac{1}{\Delta-1}\frac{dT_c}{dt}$	$-\frac{3}{2}M_c\frac{f\left(1-f^2\right)L_H}{T_c^2}\frac{1}{\Delta-1}\frac{dT_c}{dt}$
Q_k, E_k	$M_c\frac{6kT_c}{\rho D^2}$	$M_c\frac{12k}{5\rho D^4}r_c^2$

[a]Here density variations due to compressibility have been ignored. M_c is the core mass, k is the thermal conductivity, L_H is the latent heat; other terms defined in the text.

contributions may be derived using the approach given in N07. With the relationship between core growth and cooling rate derived in section 3.1, the entropy contributions E_g and E_L and their corresponding power contributions may also be derived. These quantities are summarized in Table 1, where series expansions have been truncated at terms involving $(r_c/D)^2$ (for a small body, $r_c \ll D$).

[17] Of the power terms in Table 1, the internal heating term Q_R depends on the heat production rate h (in W kg^{-1}) as expected, while the cooling term Q_s contains a small correction factor because the temperature varies with radius (equation (4)). The latent heat and gravitational power terms both depend on the core cooling rate $\frac{dT_c}{dt}$ because the rate of growth of the inner core depends on this rate (equation (7)). The latent heat terms are proportional to the latent heat of fusion L_H, while the gravitational terms depend on the fractional change in density on inner core solidification $\frac{\Delta\rho}{\rho}$ (here we assume that the light element is entirely excluded from the inner core). Both the latent heat and gravity depend on the inner core radius ($r_i = fr_c$). The quantity F in the gravitational terms is given by

$$F = \left(\frac{1}{5}+\frac{2}{15}f^5-\frac{f^2}{3}\right)\frac{f}{1-f^3} \tag{9}$$

[18] Of the five entropy terms in Table 1, the entropy per unit mass of the gravitational term E_g/M_c and the latent heat term E_L/M_c are both independent of core radius r_c, while the entropy per unit mass of the other three terms depend on r_c^2. This is an important result, because it means that for small bodies, the gravitational and latent heat contributions (if a growing inner core is present) are likely to be overwhelmingly important in determining whether a dynamo can operate. The physical reason is that the thermodynamic efficiencies of the other three terms depend on the temperature difference across the core [e.g., *Labrosse*, 2003], which becomes small as the core becomes small (equation (4)). As it turns out, the gravitational term dominates the latent heat term (see Table 1). Even for cores in Earth-mass bodies, the gravitational term is probably the dominant one in driving the dynamo [e.g., *Buffett et al.*, 1996; *Labrosse*, 2003; *Gubbins et al.*, 2004], and this becomes progressively more true for smaller bodies.

[19] In the absence of an inner core, the dynamo is driven by some combination of core cooling and internal heating. Using equation (6) and Table 1 it may be shown that the required cooling rate $\frac{dT_c}{dt}$ and heat production rate h are given by

$$-\frac{dT_c}{dt}+\frac{h}{C_p}=\frac{5D^2T_c}{2r_c^2\rho C_p}\left[\Phi_v+\frac{12}{5}\frac{kr_c^2}{D^4}\right] \tag{10}$$

Here Φ_v is the volumetric entropy production rate due to Ohmic dissipation (in W K^{-1} m^{-3}). This equation shows that as Ohmic dissipation increases or the adiabatic heat flow increases, a more rapidly cooling core (or greater internal heating) is required to drive a dynamo. As the core radius increases (or D decreases), it becomes easier to drive a dynamo, because the thermodynamic efficiency increases as the temperature difference across the core increases.

[20] For a small body with a growing inner core, the dominant effect is gravitational energy release associated with the expulsion of a light fluid from the solidifying inner core. In this case, we may write equation (6) as $E_\Phi \approx E_g - E_k$ and obtain

$$-\frac{dT_c}{dt}=\frac{T_c^2}{3\pi\rho^2G}\frac{\Delta-1}{F}\frac{\rho}{\Delta\rho}\frac{1}{D^2}\left[\Phi_v+\frac{12}{5}\frac{kr_c^2}{D^4}\right] \tag{11}$$

[21] In the presence of an inner core, the cooling rate required to drive a dynamo of a given dissipation decreases as the compositional density contrast $\Delta\rho$ increases and as the slope difference between the adiabat and melting curve decreases. In contrast to the case when an inner core is not present, the required cooling rate is independent of core radius.

3.3. Parameters

[22] Most of the parameters required are those of liquid iron or iron alloys at low pressures. The values given in Table 2 are the 1-bar liquid iron parameters given by *Anderson and Ahrens* [1994]. Liquids of different compositions (e.g., Fe-FeS) will have similar parameter values, but may yield significantly different crystallization behaviour (see section 2). We have adopted a relatively large slope difference (Δ = 1.2) so that conservatively rapid core cooling rates are required to drive a dynamo.

[23] Although there is some uncertainty in the appropriate density contrast $\Delta\rho$, the most uncertain parameter is the volumetric entropy production rate due to Ohmic dissipation, Φ_v. Estimates of the total entropy production in the Earth's core span an order of magnitude, roughly 40–400 MW/K [*Buffett*, 2002; *Labrosse*, 2003; N07]. This range gives an Ohmic dissipation of about 0.2–2 TW, assuming an effective core temperature of 5000 K, and a volumetric entropy production rate of roughly $\Phi_v = 0.2$–2×10^{-12} W K^{-1} m^{-3}. Since the estimated paleointensity of the

Table 2. Nominal Parameter Values Assumed

Qty.	Value	Units
ρ	7019	kg m^{-3}
C_p	835	J kg^{-1} K^{-1}
k	30	W m^{-1} K^{-1}
L_H	750	kJ kg^{-1}
α	9.2×10^{-5}	K^{-1}
T_c	2000	K
D	3040	km
$\Delta\rho/\rho$	0.05	-

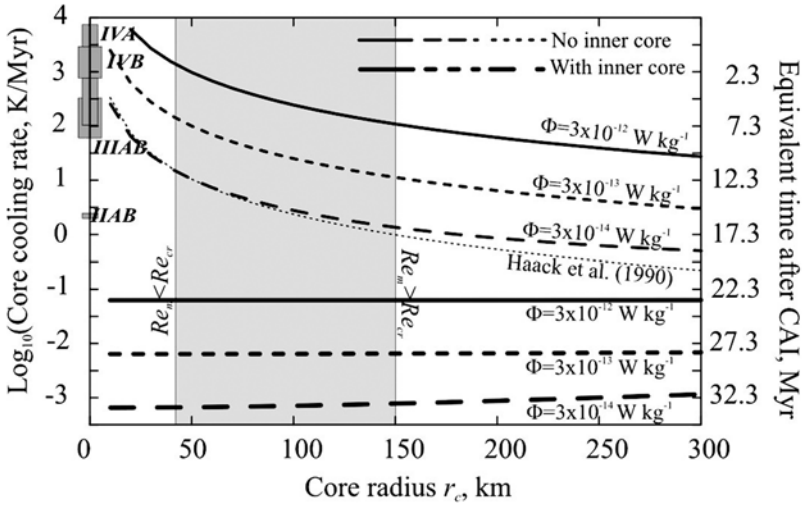

Figure 1. Core cooling rate dT_c/dt as a function of core radius r_c required to drive dynamos with different degrees of Ohmic dissipation within the core, for cases with (thick lines) and without (thin lines) an inner core. The dissipation (in W kg^{-1}) is calculated from $T_c\Phi_v/\rho$ where Φ_v is the volumetric entropy production rate (see text), $T_c = 2000$ K and $\rho = 7019$ kg m^{-3}. For the inner core we assume $r_i/r_c = 0.5$ ($F = 0.069$). The right-hand axis gives the time after CAI formation at which the heating due to ^{60}Fe decay would drive the dynamo, in the absence of any core cooling. Here an initial ^{60}Fe/^{56}Fe ratio of 10^{-6} [*Tachibana et al.*, 2006] and an energy per decay of 3 MeV are assumed. The large grey rectangle gives the region to the right of which Re_m exceeds the critical value, using equation (3) and ranges for spin period and τ of 3–100 hrs and 1–100 Myr, respectively. The small shaded boxes give the metallographic (subsolidus) cooling rate estimates for various classes of iron meteorites [from *Yang and Goldstein*, 2006; *Yang et al.*, 2008, 2009; *Chabot and Haack*, 2006], and the dotted line is the theoretical cooling rate [from *Haack et al.*, 1990].

angrite parent body field is comparable to that of the Earth [*Weiss et al.*, 2008], we will simply assume that Φ_v is similar to the terrestrial value.

4. Results

[24] The term in square brackets in equations (10) and (11) gives the relative importance of the dissipative and conductive entropy terms, E_Φ and E_k. Using the values given in Table 2 and the likely range of Φ_v derived above, the first term dominates. For the case in which there is no inner core, we can therefore write equation (10) as

$$-\frac{dT_c}{dt}+\frac{h}{C_p}\approx 25\ \mathrm{K/Myr}\left(\frac{100\ \mathrm{km}}{r_c}\right)^2\left(\frac{\Phi_v}{10^{-12}\ \mathrm{W\ K^{-1}\ m^{-3}}}\right) \quad (12)$$

[25] A cooling rate of 25 K/Myr is compatible with some estimates of asteroid core cooling rates (see below), and is equivalent to an internal heating rate of $h = 6.6 \times 10^{-10}$ W kg^{-1}. For an initial ^{60}Fe/^{56}Fe ratio of 10^{-6} [*Tachibana et al.*, 2006], this heating rate would be generated 10 Myr after CAI formation.

[26] For the case when an inner core is present, equation (11) gives

$$-\frac{dT_c}{dt}\approx 25\ \mathrm{K/Gyr}\left(\frac{\Phi_v}{10^{-12}\ \mathrm{W\ K^{-1}\ m^{-3}}}\right) \quad (13)$$

Here we assumed that $f = 0.5$ ($F = 0.069$), i.e., the inner core radius is half the core radius. Equations (12) and (13) show that for a 100 km scale core the cooling rate required to sustain a dynamo by inner core solidification is roughly three orders of magnitude slower than in the absence of a solidifying inner core. Note also that equation (13) is independent of the core radius.

[27] Figure 1 plots the core cooling rate required to sustain dynamos with different amounts of Ohmic dissipation as a function of r_c, for cases with and without an inner core. Here we are including all the terms in equation (6) and Table 1, not just the approximate equations (12) and (13). As expected, when an inner core is present the cooling rate is almost independent of r_c and is roughly three orders of magnitude smaller than when an inner core is not present. Larger amounts of Ohmic dissipation require more rapid cooling.

[28] Figure 1 also plots the minimum radius range for which the critical magnetic Reynolds number is exceeded during compositional convection (grey rectangle). Depending on the parameters adopted, the critical core radius range is ≈50–150 km (equation (3)).

[29] Rather than core cooling, in the absence of an inner core a dynamo can also be maintained by internal heating, the equivalent rate required being given by $C_p\frac{dT_c}{dt}$. The right-hand axis of Figure 1 plots the equivalent internal heating required, with the units being the time after CAI formation at which the decay of ^{60}Fe produces that amount of power. Here we are assuming an initial ^{60}Fe/^{56}Fe ratio of 10^{-6}; if the ratio were an order of magnitude lower, the times would all be decreased by 5 Myr.

[30] Figure 1 shows that with an inner core forming and expelling light material, dynamos in small bodies can be maintained by core cooling rates of order 0.1 K/Myr or less. In the absence of an inner core, the core cooling or internal heating rates required are much higher, especially for small

bodies. Nonetheless, for a 100 km scale core lacking an inner core, a moderately dissipative dynamo could be maintained entirely by ^{60}Fe decay 10 Myr after CAI formation.

[31] Figure 1 also plots the inferred metallographic (subsolidus) cooling rates for four classes of iron meteorites (shaded boxes). The IVA parent body core size is estimated at 150 ± 50 km overlain by a mantle a few km thick [*Yang et al.*, 2008], suggesting that even without an inner core a dynamo should have developed on this body. Bodies with thicker overlying mantles are likely to cool more slowly; Figure 1 also shows a theoretical core cooling rate, from *Haack et al.* [1990]. This curve suggests that without inner core growth a dynamo is only marginally likely to happen, even for the lowest entropy production rate plotted ($\Phi_v = 10^{-14}$ W K^{-1} m^{-3}). In either event, if a growing inner core is present, Figure 1 suggests that dynamo activity is hard to avoid.

5. Discussion and Conclusions

[32] The analysis above has focused on the effects of core growth from the inside out. Although it is not clear whether this is the dominant style of asteroid core crystallization [see *Chabot and Haack*, 2006], this particular mechanism is highly efficient at driving dynamos. The IVB parent body is thus particularly likely to have developed a dynamo (see section 2). Crystallization from the outside in is less well understood. It may lead to convection in a thin shell [cf. *Stanley et al.*, 2005] and certainly deserves further study [cf. *Malkus*, 1973; *Hauck et al.*, 2006]. We have also neglected complicating factors such as liquid immiscibility [*Corgne et al.*, 2008] and the behaviour of the Fe-FeS system at the eutectic.

[33] Crystallization from below is likely to drive dynamo activity in cores larger than ≈50–150 km in radius (Figure 1). In the absence of this style of crystallization, such bodies may still develop dynamos driven by ^{60}Fe heating if they formed within the first 10–20 Myr. If crystallization from below is the main dynamo driver, as for the IVB body, then one would expect asteroid/meteorite magnetic paleointensities to correlate with sulphur content: a higher sulphur content will yield a larger buoyancy flux and a stronger dynamo. On the other hand, if ^{60}Fe decay is dominant, one would expect a trend in the frequency of dynamo occurrence with semi-major axis. Bodies closer to the Sun will generally form more rapidly, undergo more radiogenic heating [*Grimm and McSween*, 1993] and thus be more likely to develop a dynamo. The spatial distribution of asteroid paleo-dynamos as measured by spacecraft [*Kivelson et al.*, 1993; *Richter et al.*, 2001] or laboratory investigations [*Gattacceca and Rochette*, 2004; *Weiss et al.*, 2008] may thus be used to test which mechanism drives these dynamos.

[34] **Acknowledgments.** I am grateful for advice from Quentin Williams and Gary Glatzmaier. Nancy Chabot and an anonymous reviewer provided useful comments.

References

Anderson, W. W., and T. J. Ahrens (1994), An equation of state for liquid iron and implications for the Earth's core, *J. Geophys. Res.*, *99*, 4273–4284.

Buffett, B. A. (2002), Estimates of heat flow in the deep mantle based on the power requirements for the geodynamo, *Geophys. Res. Lett.*, *29*(12), 1566, doi:10.1029/2001GL014649.

Buffett, B. A., H. E. Huppert, J. R. Lister, and A. W. Woods (1996), On the thermal evolution of the Earth's core, *J. Geophys. Res.*, *101*, 7989–8006.

Chabot, N. L. (2004), Sulfur contents of the parental metallic cores of magmatic iron meteorites, *Geochim. Cosmochim Acta*, *68*, 3607–3618.

Chabot, N. L., and H. Haack (2006), Evolution of asteroidal cores, in *Meteorites II*, edited by D. S. Lauretta and H. J. McSween, pp. 747–771, Univ. of Ariz. Press, Tucson.

Christensen, U. R., and J. Aubert (2006), Scaling properties of convection-driven dynamos in rotating spherical shells and application to planetary magnetic fields, *Geophys. J. Int.*, *166*, 97–114.

Corgne, A., B. J. Wood, and Y. W. Fei (2008), C- and S-rich molten alloy immiscibility and core formation of planetesimals, *Geochim. Cosmochim. Acta*, *72*, 2409–2416.

Esbensen, K. H., V. F. Buchwald, D. J. Malvin, and J. T. Wasson (1982), Systematic compositional variations in the Cape York iron meteorites, *Geochim. Cosmochim. Acta*, *46*, 1913–1920.

Garrick-Bethell, I., B. P. Weiss, D. L. Shuster, and J. Buz (2009), Early lunar magnetism, *Science*, *323*, 356–359.

Gattacceca, J., and P. Rochette (2004), Toward a robust normalized magnetic paleointensity method applied to meteorites, *Earth Planet. Sci. Lett.*, *227*, 377–393.

Grimm, R. E., and H. Y. McSween (1993), Heliocentric zoning of the asteroid belt by 26-Al heating, *Science*, *259*, 653–655.

Gubbins, D., D. Alfe, G. Masters, G. D. Price, and M. J. Gillan (2004), Gross thermodynamics of two-component core convection, *Geophys. J. Int.*, *157*, 1407–1414.

Haack, H., and E. R. D. Scott (1992), Asteroid core crystallization by inward dendritic growth, *J. Geophys. Res.*, *97*, 14,727–14,734.

Haack, H., K. L. Rasmussen, and P. H. Warren (1990), Effects of regolith/megaregolith insulation on the cooling histories of differentiated asteroids, *J. Geophys. Res.*, *95*, 5111–5124.

Hauck, S. A., II, J. M. Aurnou, and A. J. Dombard (2006), Sulfur's impact on core evolution and magnetic field generation on Ganymede, *J. Geophys. Res.*, *111*, E09008, doi:10.1029/2005JE002557.

Holme, R. (2007), Large-scale flow in the core, in *Treatise on Geophysics*, vol. 8, pp. 107–130, Elsevier, Amsterdam.

Kivelson, M. G., L. F. Bargatze, K. K. Khurana, D. J. Southwood, R. J. Walker, and P. J. Coleman (1993), Magnetic field signatures near Galileo's closest approach to Gaspra, *Science*, *261*, 331–334.

Labrosse, S. (2003), Thermal and magnetic evolution of the Earth's core, *Phys. Earth Planet. Inter.*, *140*, 127–143.

Loper, D. E. (1978), The gravitationally powered dynamo, *Geophys. J. R. Astron. Soc.*, *54*, 389–404.

Malkus, W. V. R. (1973), Convection at the melting point: A thermal history of the Earth's core, *Geophys. Fluid Dyn.*, *4*, 267–278.

Markowski, A., I. Leya, G. Quitte, K. Ammon, A. N. Halliday, and R. Wieler (2006), Correlated helium-3 and tungsten isotopes in iron meteorites: Quantitative cosmogenic corrections and planetesimal formation times, *Earth Planet. Sci. Lett.*, *250*, 104–115.

Nimmo, F. (2007), Energetics of the core, in *Treatise on Geophysics*, vol. 8, pp. 31–65, Elsevier, Amsterdam.

Olson, P., and U. R. Christensen (2006), Dipole moment scaling for convection-driven planetary dynamos, *Earth Planet. Sci. Lett.*, *250*, 561–571.

Richter, I., D. E. Brinza, M. Cassel, K.-H. Glassmeier, F. Kuhnke, G. Musmann, C. Othmer, K. Schwingenschuh, and B. T. Tsurutani (2001), First direct magnetic field measurements of an asteroidal magnetic field: DS1 at Braille, *Geophys. Res. Lett.*, *28*, 1913–1916.

Runcorn, S. K. (1994), On the origin of the supposed magnetization of Gaspra, *Meteoritics*, *29*, 525.

Stanley, S., J. Bloxham, W. E. Hutchison, and M. T. Zuber (2005), Thin shell dynamo models consistent with Mercury's weak observed magnetic field, *Earth Planet. Sci. Lett.*, *234*, 27–38.

Stegman, D. R., A. M. Jellinek, S. A. Zatman, J. R. Baumgardner, and M. A. Richards (2003), An early lunar core driven by thermochemical mantle convection, *Nature*, *421*, 143–146.

Stevenson, D. J. (2003), Planetary magnetic fields, *Earth Planet. Sci. Lett.*, *208*, 1–11.

Tachibana, S., G. R. Huss, N. T. Kita, G. Shimoda, and Y. Morishita (2006), Fe-60 in chondrites: Debris from a nearby supernova in the early solar system?, *Astrophys. J. Lett.*, *639*, 87–90.

Wasson, J. T., Y. Matsunami, and A. E. Rubin (2006), Silica and pyroxene in IVA irons: Possible formation of the IVA magma by impact melting and reduction of L-LL chondrite materials followed by crystallization and cooling, *Geochim. Cosmochim. Acta*, *70*, 3149–3172.

Weiss, B. P., J. S. Berdahl, L. Elkins-Tanton, S. Stanley, E. A. Lima, and L. Carporzen (2008), Magnetism on the angrite parent body and the early differentiation of planetesimals, *Science*, *322*, 713–716.

Yang, J., and J. I. Goldstein (2006), Metallographic cooling rates of the IIIAB iron meteorites, *Geochim. Cosmochim. Acta*, *70*, 3197–3215.

Yang, J., J. I. Goldstein, and E. R. D. Scott (2008), Metallographic cooling rates and origin of the IVA iron meteorites, *Geochim. Cosmochim. Acta*, *72*, 3043–3061.

Yang, J., J. I. Goldstein, J. R. Michael, and P. G. Kotula (2009), Composition and thermal history of the IVB iron meteorites, *Lunar Planet. Sci.*, *XL*, Abstract 1186.

F. Nimmo, Department of Earth and Planetary Sciences, University of California, 1156 High Street, Santa Cruz, CA 95064, USA. (fnimmo@es.ucsc.edu)